THE JOURNAL OF BIOLOGICAL CHEMISTRY VOL. 286, NO. 27, pp. 23911–23919, July 8, 2011

Atypical Cristae Morphology of Human Syncytiotrophoblast Mitochondria

*ROLE FOR COMPLEX V**

Received for publication, April 15, 2011 Published, JBC Papers in Press, May 13, 2011, DOI 10.1074/jbc.M111.252056

Daniela De Los Rios Castillo[‡], Mariel Zarco-Zavala[§], Sofia Olvera-Sanchez[‡], Juan Pablo Pardo[‡], Oscar Juarez[¶], Federico Martinez[‡], Guillermo Mendoza-Hernandez[‡], José J. García-Trejo[§], and Oscar Flores-Herrera[‡1]

From the [‡]Department of Biochemistry and Molecular Biology, Medicine Faculty, National Autonomous University of Mexico, 04510 Mexico City, Mexico, the [§]Department of Biology, Chemistry Faculty, National Autonomous University of Mexico, 04510 Mexico City, Mexico, and the [¶]Biology Department, Center for Biotechnology and Interdisciplinary Studies, Rensselaer Polytechnic Institute, Troy, New York 12180

Mitochondrial complexes I, III_2, and IV from human cytotrophoblast and syncytiotrophoblast associate to form supercomplexes or respirasomes, with the following stoichiometries: I_1:$(III_2)_1$ and I_1:$(III_2)_{1-2}$:IV_{1-4}. The content of respirasomes was similar in both cell types after isolating mitochondria. However, syncytiotrophoblast mitochondria possess low levels of dimeric complex V and do not have orthodox cristae morphology. In contrast, cytotrophoblast mitochondria show normal cristae morphology and a higher content of ATP synthase dimer. Consistent with the dimerizing role of the ATPase inhibitory protein (IF_1) (García, J. J., Morales-Ríos, E., Cortés-Hernandez, P., and Rodríguez-Zavala, J. S. (2006) *Biochemistry* 45, 12695–12703), higher relative amounts of IF_1 were observed in cytotrophoblast when compared with syncytiotrophoblast mitochondria. Therefore, there is a correlation between dimerization of complex V, IF_1 expression, and the morphology of mitochondrial cristae in human placental mitochondria. The possible relationship between cristae architecture and the physiological function of the syncytiotrophoblast mitochondria is discussed.

Oxidative phosphorylation, the main source of ATP in aerobic cells, relies on the activity of two components, the oxidative and the phosphorylation systems. The oxidative system (respiratory chain) couples redox reactions to the production of a proton electrochemical gradient, which drives the synthesis of ATP by the phosphorylation system (F_0F_1-ATP synthase and the ADP and phosphate carriers). Because the respiratory complexes of the electron transport chain can be isolated, preserving its functional properties, it was generally accepted that these complexes exist as isolated entities that can move laterally and independently in the mitochondrial inner membrane (1–3).

However, during the last decade, a large number of studies have revealed the strong association between the electron transport complexes into the so-called respiratory supercomplexes. These associations are widespread and can be found in a variety of different mitochondria, including those of vertebrates (4, 5), plants (6), and fungi (4), and in the respiratory chains of some bacteria such as *Paracoccus denitrificans* (7), where by contrast, the complex V or ATP synthase is monomeric (8, 9). However, some major differences are evident; for instance, in plants, the major supercomplex is the I-III_2 (10), whereas in mammals, other supercomplexes can be found, such as the I-III_2, I-III_2-IV, I-III_2-IV_2, and I-III_2-IV_4 (4, 5). The evidence indicates that supercomplexes may have significant roles in cell physiology, such as an increase in complex stability, substrate channeling, and reduction of reactive oxygen species production.

On the other hand, mitochondrial F_0F_1 ATP synthase self-associates in dimeric and oligomeric structures in *Bos* (8, 11, 12), *Saccharomyces cerevisiae* (4, 13, 14), *Polytomella sp.* (15, 16), and *Chlamydomonas reinhardtii* (17, 18). The F_0F_1-ATP synthase dimer (V_2) seems to be closely related with the mitochondrial architecture. In particular, it has been suggested that the presence of cristae in mitochondria depends on the ability of complex V to form dimers (11, 19–21). The factors involved in the dimerization process appear to be different in several organisms; in yeast mitochondria, the F_0F_1 dimer is stabilized by F_0 subunits e and g (22–25), whereas in the chlorophycean algae *C. reinhardtii* and *Polytomella sp.*, the ASA1–8 subunits are involved in this process (16, 17). Additionally, in bovine and rat mitochondria, this dimerizing role is also accomplished by the inhibitor protein (IF_1)[2] (12) along with the dimerizing F_0 subunits; this is in contrast with yeast IF_1, which does not seem to be essential for F_0F_1 dimerization (26).

Studies on the supramolecular associations of the oxidative phosphorylation system have been typically performed in mitochondria of aerobic cells, whose main role is the synthesis of ATP. Our group has been interested in the physiology of mitochondria from steroidogenic tissues, such as human placenta. The latter contains two functionally different layers, the

* This work was supported by Research Grants IN238402 (to O. F.-H.), IN217609 (to F. M.), and IN213809 (to J. J. G.-T.) from Dirección General de Asuntos del Personal Académico (DGAPA) from Universidad Nacional Autónoma de México and Grants 52211 (to O. F.-H.) and 59855 (to J. P. P.) from Consejo Nacional de Ciencia y Tecnología (CONACyT).

[1] To whom correspondence should be addressed: Departamento de Bioquímica, Facultad de Medicina, Universidad Nacional Autonoma de México, Apdo Postal 70-159, Coyoacan 04510, Mexico, D. F., México; Tel.: 55-56232510; Fax: 55-56162419; E-mail: oflores@bq.unam.mx.

[2] The abbreviations used are: IF_1, inhibitor protein; DCPIP, dichlorophenolindophenol; DDM, dodecyl-β-D-maltoside; OSCP, osteoblast-specific cysteine-rich protein; BN-PAGE, Blue Native PAGE; CN-PAGE, Clear Native PAGE; Bis-Tris, 2-(bis(2-hydroxyethyl)amino)-2-(hydroxymethyl)propane-1,3-diol; Tricine, *N*-[2-hydroxy-1,1-bis(hydroxymethyl)ethyl]glycine; CAPS, 3-(cyclohexylamino)propanesulfonic acid.

cytotrophoblast and the syncytiotrophoblast. The cytotrophoblast shows mitotic activity and is in contact with the endometrium; by contrast, the syncytiotrophoblast is facing the uterus, has no mitotic activity, and displays a high steroidogenic activity, with progesterone as the main product. We have described previously that the morphology of the syncytiotrophoblast mitochondria is far from typical, showing a highly condensed matrix and an irregular folding of the mitochondrial inner membrane (27). The present study represents the first report addressing the presence and analysis of respiratory chain complexes and supercomplexes of human placental mitochondria and their role in cristae morphology. It is shown that the atypical morphology of the syncytiotrophoblast mitochondria correlates with low contents of dimeric F_0F_1-ATP synthase and of the inhibitory IF_1 subunit, confirming the key role played by these two factors in determining mitochondrial cristae morphology.

EXPERIMENTAL PROCEDURES

Isolation of Human Cytotrophoblast and Syncytiotrophoblast Mitochondria—Full term human placenta was collected immediately after normal delivery. Mitochondria were prepared as described previously (27). To purify mitochondria of cytotrophoblast or syncytiotrophoblast, the enriched mitochondrial suspension was loaded on a 35% sucrose solution (25 ml) and centrifuged at 15,000 × *g* for 45 min, at 4 °C. The two mitochondrial fractions were collected and centrifuged at 16,000 times] *g* for 15 min at 4 °C, and the mitochondrial pellet was resuspended in 250 mM sucrose, 10 mM Tris (pH 7.4) and stored at −70 °C until use. Protein concentration was measured as reported (28, 29).

Mitochondrial Oxygen Consumption—Oxygen uptake was estimated polarographically using a Clark type electrode in a mixture containing 250 mM sucrose, 10 mM HEPES, pH 7.4, 1 mM EGTA, 1 mM EDTA, 10 mM succinate, 10 mM KH_2PO_4, 5 mM $MgCl_2$, 0.2% bovine serum albumin, and 1 mg/ml cytotrophoblast or syncytiotrophoblast mitochondrial protein (30). Temperature was set at 37 °C, and oxygen consumption was stimulated by the addition of 300–500 nmol of ADP.

Mitochondrial Enzyme Activity Determinations—Activities of complex I (NADH:DCPIP oxidoreductase) and complex II (succinate:DCPIP oxidoreductase) were determined spectrophotometrically at 600 nm by following the reduction of the artificial electron acceptor 2,6-dichlorophenol-indophenol (DCPIP; 50 μM; ϵ_{DCPIP} = 21 $mM^{-1}cm^{-1}$). Mitochondria permeabilized with 0.01% Triton X-100 were incubated in 30 mM KH_2PO_4, 5 mM $MgCl_2$, 1 mM EGTA, 120 mM KCl, pH 7.4, and either 500 μM NADH (complex I) or 2 mM succinate (complex II). The protein concentration of cytotrophoblast or syncytiotrophoblast mitochondria was 50 μg/ml, and the reaction was started by the addition of NADH or succinate.

ATP synthesis by complex V was measured at 37 °C using an assay coupled to the reduction of $NADP^+$ ($\epsilon_{340\,nm}$ = 6.2 $mM^{-1}cm^{-1}$). The reaction mixture contained 0.5 mM $NADP^+$, 1 mM ADP, 6 units/ml glucose-6-phosphate dehydrogenase, 16 units/ml hexokinase, 10 mM succinate, 100 μM P^1, P^5-Di(adenosine-5′)pentaphosphate penta-ammonium, 10 mM glucose, 150 mM sucrose, 5 mM $MgCl_2$, 20 mM Tris/HCl, and 20 mM KH_2PO_4, pH 7.5. ATP synthesis was started by the addition of cytotrophoblast or syncytiotrophoblast mitochondria (50 μg/ml). The values reported were obtained by subtracting the rate of ATP synthesis in the presence of oligomycin (5 μg/mg mitochondrial protein) from the amount of ATP synthesis in the control conditions.

Mitochondrial Progesterone Synthesis—Progesterone synthesis was determined at 37 °C as reported previously (30) in 120 mM KCl, 10 mM MOPS, 0.5 mM EGTA, 10 mM isocitrate, 4 μg of aprotinin/ml, 1 μM leupeptin, 5 mM KH_2PO_4, pH 7.4, in a final volume of 500 μl with 1 mg/ml cytotrophoblast or syncytiotrophoblast mitochondrial protein. Where indicated, 25 μM 22(*R*)-hydroxy-cholesterol was added. After a 60-min incubation, the reaction was stopped with 50 μl of methanol, and progesterone was determined by a radioimmunoassay kit (Diagnostic Systems Laboratories, Inc., Webster, TX) according to the manufacturer's instructions. The concentration of progesterone at time 0 was subtracted from the amount of progesterone at 60 min, and this net value of progesterone synthesis was reported.

Electron Microscopy—Samples for transmission electron microscopy were fixed in 2% glutaraldehyde, post-fixed with osmium tetroxide, and sequentially dehydrated with increasing concentrations of ethanol. Finally, the samples were embedded in an epoxy resin (31). Sections were cut and stained with uranyl acetate and lead citrate and observed under a Jeol electron microscope, operated at 60 kV. Placental tissue was fixed for immunogold studies with 4% paraformaldehyde, 0.2% glutaraldehyde, and phosphate-buffered saline (31).

Sample Preparation for Native Electrophoresis—The respiratory complexes from either cytotrophoblast or syncytiotrophoblast mitochondria were resolved by native PAGE following the general procedures reported previously (32, 33) with minor modifications. Briefly, cytotrophoblast (2 mg) or syncytiotrophoblast (2 mg) mitochondria were suspended in 50 mM Bis-Tris and 500 mM 6-aminocaproic acid, pH 7.0, and solubilized by adding dodecyl-β-D-maltoside or digitonin, at detergent/protein ratios ranging from 0.5 to 10 (g/g), in a final volume of 200 μl. The mixtures were incubated for 30 min at 4 °C and centrifuged at 100,000 times] *g* for 30 min at 4 °C. The supernatants were recovered and immediately loaded on a linear polyacrylamide gradient gel (5–10% or 3.25–7.5%) for Blue Native PAGE (BN-PAGE) or Clear Native PAGE (CN-PAGE) (34). The molecular weight of each respiratory complex or supercomplex was estimated by using the bovine mitochondrial complexes as standard.

In-gel Catalytic Activity Assays—The in-gel activity assays were performed as described by Wittig *et al.* (34). Gel strips were assayed for complex I activity (NADH:methylthiazolyldiphenyl tetrazolium bromide reductase), complex II activity (succinate:methylthiazolyldiphenyl tetrazolium bromide reductase), and complex IV activity (cytochrome *c*:diaminobenzidine reductase). In all cases, the assays were performed at 20–25 °C and stopped with 50% methanol, 10% acetic acid, after 10–25 min.

To estimate the in-gel ATP hydrolysis activity of monomeric and dimeric complex V and of the F_1-ATPase subcomplex, gel strips were preincubated in 50 mM glycine (adjusted to pH 8.0

with triethanolamine) for 2 h at 37 °C in the presence or absence of the complex V inhibitor oligomycin (5 μg/ml). The equilibration solution was discarded, and the gel strips were then added into the assay buffer (50 mM glycine, adjusted to pH 8.0 with triethanolamine, 10 mM $MgCl_2$, 0.2% $Pb(NO_3)_2$, and 8 mM ATP), with or without 5 μg/ml oligomycin. ATP hydrolysis correlated with the development of white lead phosphate precipitates. The reaction was stopped using 50% methanol, and subsequently the gel was transferred to water and scanned against a dark background as described previously (11, 35).

Two-dimensional Tricine-SDS Gel Electrophoresis and Western Blot Analysis—Proteins of a gel lane excised from native PAGE were separated by two-dimensional Tricine-SDS-PAGE according to Ref. 32 on a 16% polyacrylamide gel under denaturing conditions. Afterward, the proteins were stained with either Coomassie Brilliant Blue R-125 or silver using a commercial kit (Bio-Rad). Alternatively, the gels were electrotransferred to polyvinylidene difluoride membrane (Immobilon P; Millipore, Bedford, MA) in a semidry electroblotting system (Bio-Rad) at 25 V for 50 min or 2 h at 100 mA in a buffer containing 100 mM CAPS, 10% methanol (pH = 11). Membranes were blocked in 500 mM NaCl, 0.05% Tween 20, and 20 mM Tris base, pH 7.5 (TTBS buffer) containing 5% blotting grade blocker nonfat dry milk (Bio-Rad). The antibodies used were anti-α subunit polyclonal antibody (1:10,000), anti-β subunit antibody (1:250), anti-OSCP subunit antibody (1:1000), and anti-IF_1 monoclonal antibody (1:10,000). Membranes were incubated for 1 h with the primary antibody in TTBS buffer and washed thoroughly, and the immunoreactive bands were visualized with the enhanced chemiluminescence assay (Amersham Biosciences) according to the manufacturer's instructions, using horseradish peroxidase-conjugated goat anti-mouse IgG (Pierce) at a dilution of 1:35,000, and the densitometric analyses were performed with the Alpha-DigiDoc 1000 software (AlphaEaseFC™ from Alpha Innotech Corp.). The intensities of subunits were measured by peak integration after densitometry analyses.

Tandem Mass Spectrometry (LC/ESI-MS/MS)—The protein spots (indicated by numbers in Figs. 2*A* and 3*C* and Table 2) were excised from the Coomassie Brilliant Blue R-125-stained SDS gels, distained, reduced, carbamidomethylated, and digested with modified porcine trypsin (Promega, Madison, WI). Peptide mass spectrometric analysis was carried out using a 3200 Q TRAP hybrid tandem mass spectrometer (Applied Biosystems/MDS Sciex, Concord, Ontario, Canada), equipped with a nanoelectrospray ion source (NanoSpray II) and a MicroIonSpray II head (36). The instrument was coupled on-line to a nanoAcquity Ultra Performance LC system supplied by Waters (Waters Corp., Milford, MA). Briefly, spectra were acquired in automated mode using information-dependent acquisition. Precursor ions were selected in Q1 using the enhanced MS mode as survey scan. The enhanced MS mode was followed by an enhanced resolution scan of the three most intense ions at the low speed of 250 atomic mass units/s to determine the ion charge states and afterward by an enhanced product ion scan. The precursor ions were fragmented by collisionally activated dissociation in the Q2 collision cell. The fragment ions generated were captured and mass analyzed in the Q3 linear ion trap.

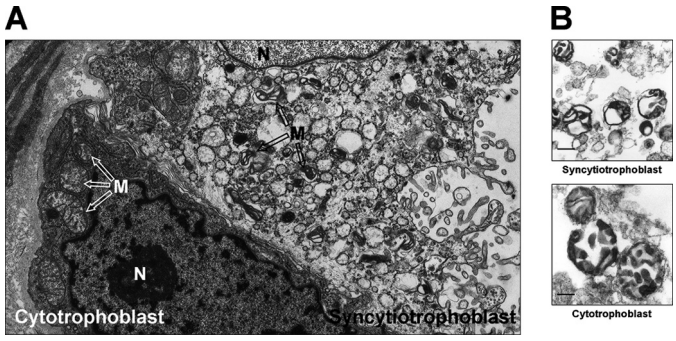

FIGURE 1. **Ultrastructure of human syncytiotrophoblast and cytotrophoblast cells.** *A*, electron micrograph of term placenta villus showing syncytiotrophoblast and underlying cytotrophoblast. *N*, nucleus; *M*, mitochondria. Magnification, 10,000 ×. *B*, isolated mitochondria from human cytotrophoblast and syncytiotrophoblast. *Scale bar*, 200 nm.

Database searching and protein identification were performed with the MS/MS spectra data sets using the MASCOT search algorithm (version 1.6b9, Matrix Science, London, UK). Mass tolerances of 0.5 Da for the precursor and 0.3 Da for the fragment ion masses were used. Carbamidomethyl-cysteine was the fixed modification, and one missed cleavage for trypsin was allowed. Searches were conducted using the Human subset of the NCBInr database (www.ncbi.nih.gov). Protein identifications were accepted when at least two MS/MS spectra matched at 95% confidence level ($p < 0.05$).

Materials—Analytical grade reagents were purchased from Sigma, Merck (Darmstadt, Germany), and Bio-Rad. Antibodies were purchased from Santa Cruz Biotechnology and MitoSciences®.

RESULTS

Human Placental Mitochondria Architecture—Transmission electron micrographs of term placenta sections revealed two morphological types of mitochondria in the trophoblast cells (Fig. 1*A*). Large mitochondria were observed in the cytotrophoblast cells, whose morphology is similar to that of typical liver mitochondria, containing lamellar (and presumably tubular) cristae in an orthodox configuration. In contrast, the syncytiotrophoblast contained smaller mitochondria with a condensed matrix and cristae composed by vesicular regions connected by narrow tubules. The larger cytotrophoblast mitochondria had a round shape, whereas the syncytiotrophoblast mitochondria display an irregular shape with protuberances of the outer and inner membranes. Isolated cytotrophoblast and syncytiotrophoblast mitochondria only partially retained these structural characteristics (Fig. 1*B*); in particular, the isolated cytotrophoblast mitochondria had partially lost the original cristae configuration seen *in situ* (Fig. 1*A*).

Physiological State of Cytotrophoblast and Syncytiotrophoblast Mitochondria—To determine the functional integrity of isolated cytotrophoblast and syncytiotrophoblast mitochondria, respiratory rates and respiratory controls were calculated from oxygen uptake traces using succinate as substrate (Table 1). Values of respiratory control ranged between 2.85 and 12, higher than those previously reported for this tissue (37); ATP

TABLE 1
Bioenergetics and steroidogenic parameters of cytotrophoblast and syncytiotrophoblast mitochondria

	Mitochondria	
	Cytotrophoblast	Syncytiotrophoblast
Complex activities[a]		
Complex I	113 ± 40 μM/mg/min	110 ± 46 μM/mg/min
Complex II	12 ± 6 μM/mg/min	14 ± 4 μM/mg/min
Complex V	151 ± 16 nmol/mg/min	153 ± 13 nmol/mg/min
Respiratory control[b]		
Placenta 1	2.93 ± 0.25	6.00 ± 1.70
Placenta 2	2.85 ± 0.15	3.31 ± 0.44
Placenta 3	4.48 ± 1.59	12.00 ± 5.3
Progesterone synthesis[c]		
Control	3.6 ± 1.34 of ng of progesterone/mg/min	35.7 ± 0.90 of ng of progesterone/mg/min
+22(*R*)-hydroxy-cholesterol	10.1 ± 3.95 ng of progesterone/mg/min	92.2 ± 3.40 of ng of progesterone/mg/min

[a] Specific activities from complexes I and II were measured spectrophotometrically in sonicated mitochondria:complex I, NADH:DCPIP oxide reductase; complex II, and succinate:DCPIP oxide reductase. Specific complex V activity was determined in intact mitochondria as ATP synthesis.
[b] Respiratory control = oxygen uptake ratio to state 3 (natoms g of oxygen)/oxygen uptake ratio to state 4 (natoms g of oxygen).
[c] Progesterone synthesis was determined as described in experimental procedure. The 22(*R*)-hydroxy-cholesterol was used to assess maximal steroidogenic activity. Values shows here are the mean ± S.D. from seven to eight determinations, from eight different placental tissues.

synthesis by complex V was 151 ± 16 and 153 ± 13 nmol/mg/min for cytotrophoblast and syncytiotrophoblast mitochondria, respectively, suggesting coupling of mitochondrial respiration and ATP synthesis. In addition, we obtained an activity of 113–110 μmol/mg/min for the NADH:DCPIP oxide reductase activity (complex I) and 12–14 μmol/mg/min for the succinate:DCPIP oxide reductase activity (complex II) (Table 1). These results indicate the presence of functional mitochondria in both cell types, retaining the ability to increase the consumption of oxygen and the synthesis of ATP upon the addition of ADP.

Human placental mitochondria are steroidogenic organelles that synthesize progesterone due to the presence of the 3-β-hydroxy steroid dehydrogenase in their inner membrane (27, 38, 39). Because there are two types of mitochondria, its steroidogenic activity was determined. Table 1 shows that synthesis of progesterone by syncytiotrophoblast mitochondria (35.7 ± 0.9 ng of progesterone/mg/min) was 10-fold higher than that of cytotrophoblast mitochondria (3.6 ± 1.34 ng of progesterone/mg/min). In both cases, 22(*R*)-hydroxy-cholesterol, a soluble substrate used to assess maximal steroidogenic activity (40), increased steroidogenic activity to 92.2 ± 3.4 and 10.1 ± 3.95 ng of progesterone/mg/h in syncytiotrophoblast and cytotrophoblast mitochondria, respectively. These results are in accordance with the specialized role of each placental tissue (27) and support that isolated mitochondria retain their physiological function.

Identification of Respiratory Supercomplexes in Mitochondria from Cytotrophoblast and Syncytiotrophoblast Cells—To investigate the optimal condition for the separation of mitochondrial complexes and supercomplexes, isolated mitochondria from both cytotrophoblasts and syncytiotrophoblasts were solubilized by varying concentrations of either digitonin or dodecyl-β-D-maltoside (DDM). Results showed that 1–2 g of DDM/g of mitochondrial protein allowed the solubilization of the respiratory chain complexes in their monomeric state (Fig. 2*A*), except for complex III, which exists as a stable dimer. BN-PAGE allowed the resolution of all the complexes of the oxidative phosphorylation system (Fig. 2*A*). The identity and position of complexes I, II, IV, and V on gels were determined using specific reactions for these complexes (Fig. 2*A*). The molecular mass estimated for each complex was: complex I, 1000 kDa; complex V, 750 kDa; complex III_2, 500 kDa; complex IV, 200 kDa; and complex II, 130 kDa. In addition, the identity of each complex was confirmed by their known subunit composition upon resolution on two-dimensional SDS-PAGE and by identification of subunits by mass spectrometry (Fig. 2*B* and Table 2). Identical results were obtained for cytotrophoblast and syncytiotrophoblast mitochondria (Table 2).

With digitonin as the solubilizing agent, it was possible to isolate the mitochondrial respiratory chain components as individual entities or as supercomplexes. The optimal digitonin/mitochondrial protein ratio was found between 1.5 and 10. However, the abundance of some supercomplexes decreased slightly at higher detergent/protein ratios; therefore, all further experiments were carried out with a digitonin/protein ratio of 1.5 (g/g). The identity and position of the individual complexes I, V, IV, and II, as well as the composition of supercomplexes named a–e, were determined using specific reactions for these complexes (Fig. 3*A*). The molecular mass of each individual complex was essentially identical to that obtained using DDM for the solubilization process (Table 2). However, the presence of five different supercomplexes was clearly evident in the gel. To resolve the composition of these supercomplexes, BN-PAGE was carried out in 3.25–7.5% linear polyacrylamide gradient gels. As shown in Fig. 3*B*, about 70% of the NADH:methylthiazolyldiphenyl tetrazolium bromide oxidoreductase activity was located at the position corresponding to the supercomplexes, whereas the cytochrome *c*:diaminobenzidine oxidoreductase activity was detected only in three of them (c–e) (Fig. 3*B*). Occurrence of complex III was determined by two-dimensional SDS-PAGE followed by spot identification by mass spectrometry (Fig. 3*C*). The molecular masses estimated for the supercomplexes and their possible stoichiometry were: a = 1,300 kDa (I_1:III_2); b = 1,500 kDa (I_1:III_2); c = 1,700 kDa (I_1:III_2:IV_1); d = 2,000 kDa (I_1:III_2:IV_{2-3}); and e = 2,300 kDa (I_1:$(III_2)_{1-2}$:IV_{1-4}).

Monomeric and Dimeric F_0F_1-ATP Synthase in Mitochondria from Cytotrophoblast and Syncytiotrophoblast—Solubilization of cytotrophoblast and syncytiotrophoblast mitochondria with digitonin (1.5 mg/mg of protein) allowed the visualization of the activity of the monomeric (V) and dimeric

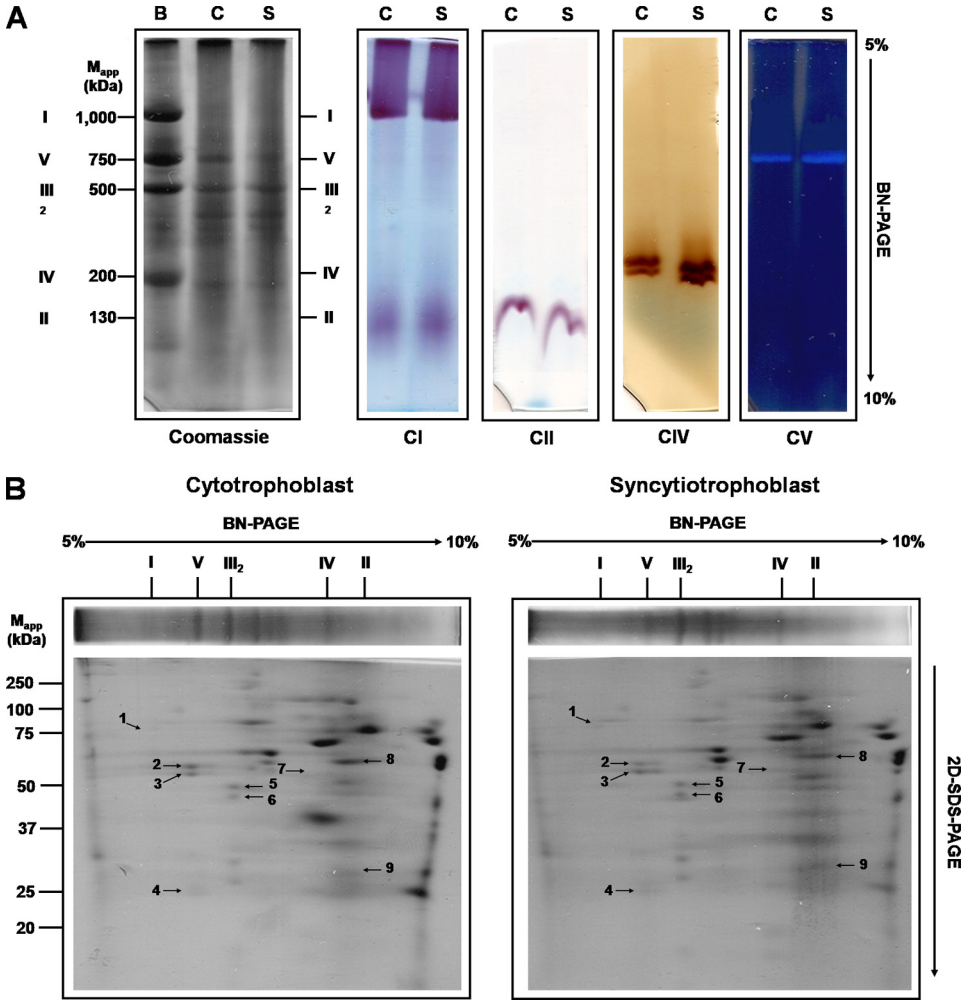

FIGURE 2. **In-gel activity and identification of DDM-solubilized mitochondrial OXPHOS complexes from cytotrophoblasts and syncytiotrophoblasts in native gels.** Mitochondria were solubilized using DDM (1–2 g/g of protein), and respiratory complexes were separated by BN-PAGE followed by two-dimensional SDS-PAGE. *A*, BN-PAGE. The *left panel* shows the Coomassie Brilliant Blue R-125-stained native gel strips; *CI*, *CII*, *CIV*, and *CV* correspond to in-gel catalytic activity assays of complexes I, II, IV, and V. Bovine heart mitochondria were solubilized with DDM as described under "Experimental Procedures" and used as standard. *B*, *C*, and *S* represent bovine, cytotrophoblast, and syncytiotrophoblast mitochondria, respectively. *B*, for identification of respiratory chain complex subunits, proteins were resolved by two-dimensional SDS-PAGE, and their identities were determined using the MALDI-TOF technique (indicated by the numbers shown in Table 2).

TABLE 2

Molecular mass and subunit identity of cytotrophoblast and syncytiotrophoblast mitochondrial respiratory complexes

The molecular mass of the complexes was determined by BN-PAGE using mitochondrial respiratory complexes from heart bovine as standard. The subunit molecular mass was determined by two-dimensional SDS-PAGE. The identity of each protein spot was determined. The number into parenthesis in subunit identity column is the same of Figs. 2*B* and 3*C*.

Complexes		Subunit		
Identity	Molecular mass determined	Identity	Molecular mass determined	Accession number
	kDa		*kDa*	
I	1000	NDUFS1 (1)	75	NP_004997
		NDUFA9 (10)	39	NP_004993
		NDUFS3 (11)	26	NP_004542
II	130	SDHA (8)	68	NP_004159
		SDHB (9)	30	NP_002991
III	500	UQCRC1 (5)	49	NP_003356
		UQCRC2 (6)	47	NP_003357
IV	200	MT-COI (7)	56	YP_003024028
V	750	ATP5A1 (2)	55	NP_001001937
		ATP5B (3)	52	NP_001677
		ATP5O (4)	21	NP_001688
		ATPIF1 (12)	10	NP_057395

(V_2) forms of the F_0F_1-ATP synthase complex in BN-PAGE (Fig. 3*A*). It has been reported that the ATPase activity of the F_0F_1 complex is affected by the Coomassie Brilliant Blue R-125 used in the BN-PAGE (41); therefore, we used the CN-PAGE to visualize the F_0F_1 complex activity (Fig. 3*A*, *right panel*). In accordance with a previous study (42), the F_0F_1-ATP synthase is present in two forms, a monomeric complex of about 750 kDa and a dimeric complex of about 1500 kDa. In cytotrophoblast mitochondria, the in-gel ATPase activity of V, evidenced as a white precipitate, was greater than that of V_2 (Fig. 3*A*, *right panel*), whereas in syncytiotrophoblast mitochondria, this difference in ATPase activity was much larger. Indeed, in some syncytiotrophoblast mitochondria preparations, the ATP synthase activity was represented by the monomeric form exclusively. Thus, the V_2 ATPase activity for the cytotrophoblast mitochondria was higher than that of syncytiotrophoblast mitochondria. Because the differences in intensity of in-gel ATPase bands may result from different specific activities, two-dimensional SDS-PAGE was carried out after BN-PAGE to

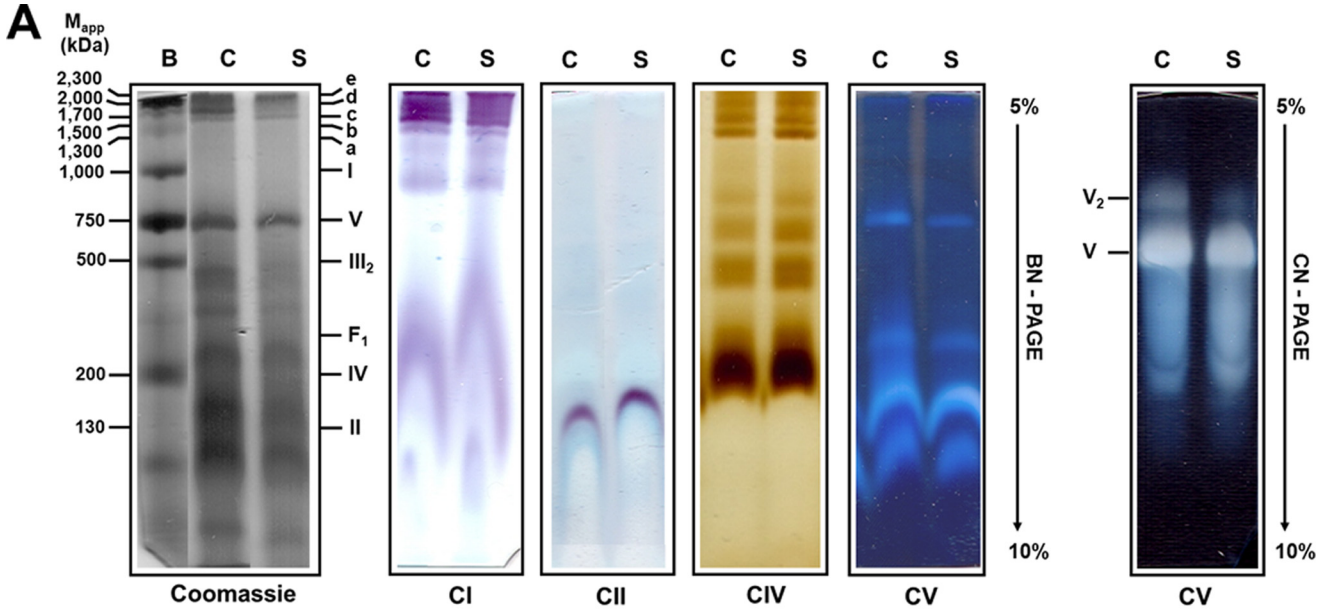
A
M_{app} (kDa)
B C S
2,300
2,000
1,700
1,500
1,300
1,000
750
500
200
130
e
d
c
b
a
I
V
III_2
F_1
IV
II
Coomassie
C S
CI
C S
CII
C S
CIV
C S
CV
5%
10%
BN - PAGE
C S
CV
5%
10%
CN - PAGE
V_2
V

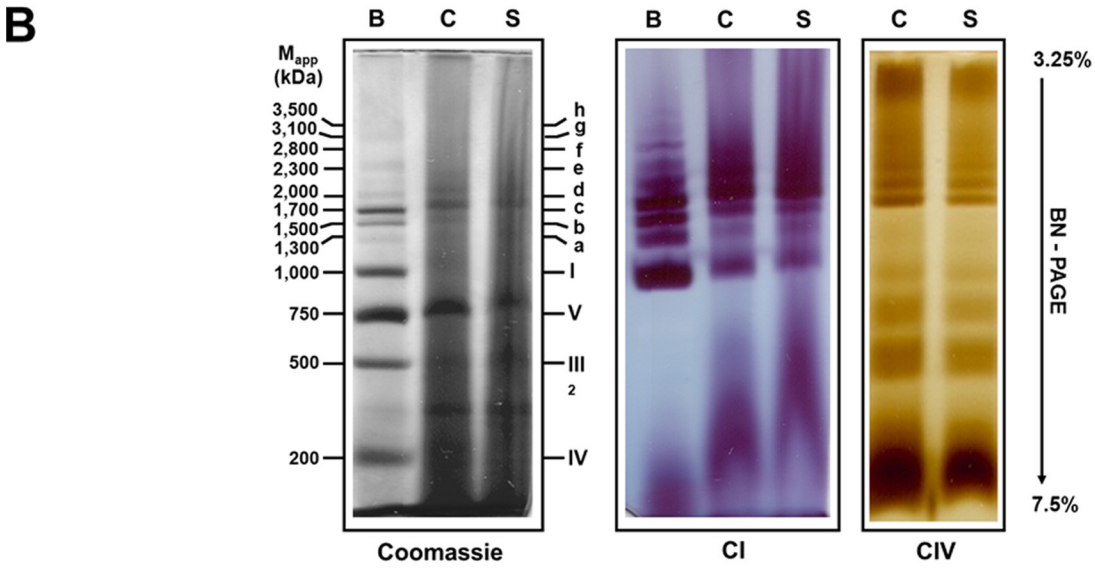
B
B C S
M_{app} (kDa)
3,500
3,100
2,800
2,300
2,000
1,700
1,500
1,300
1,000
750
500
200
h
g
f
e
d
c
b
a
I
V
III
2
IV
Coomassie
B C S
CI
C S
CIV
3.25%
7.5%
BN - PAGE

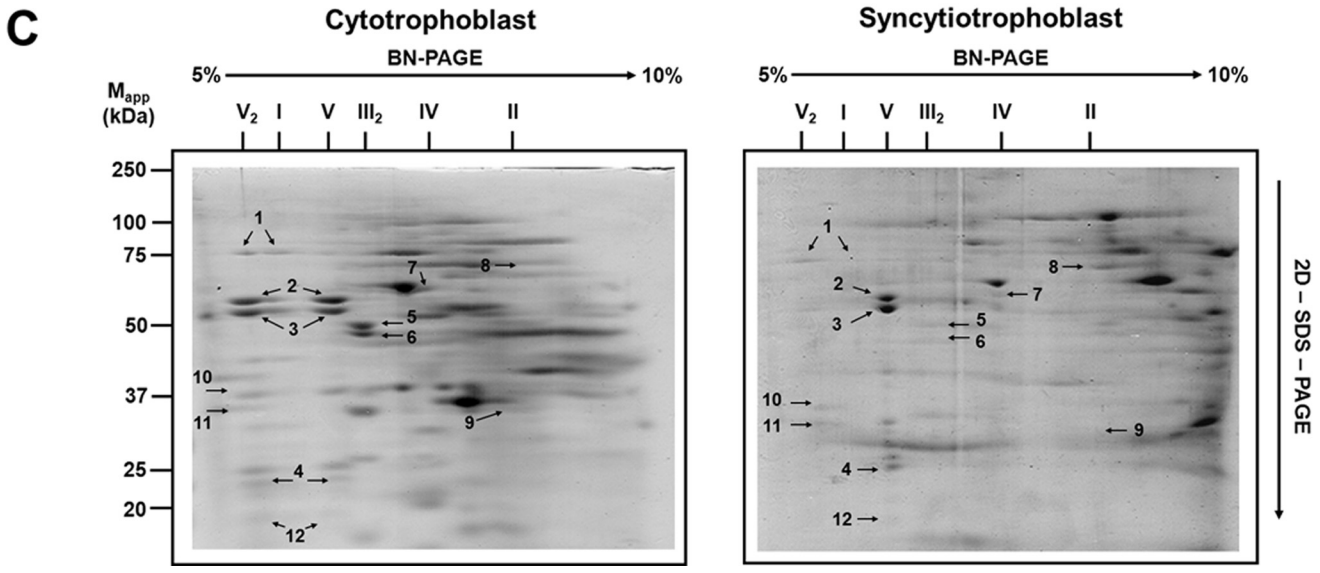
C
Cytotrophoblast
BN-PAGE
5%
10%
M_{app} (kDa)
V_2 I V III_2 IV II
250
100
75
50
37
25
20
1
2
3
4
5
6
7
8
9
10
11
12
Syncytiotrophoblast
BN-PAGE
5%
10%
V_2 I V III_2 IV II
1
2
3
4
5
6
7
8
9
10
11
12
2D – SDS – PAGE

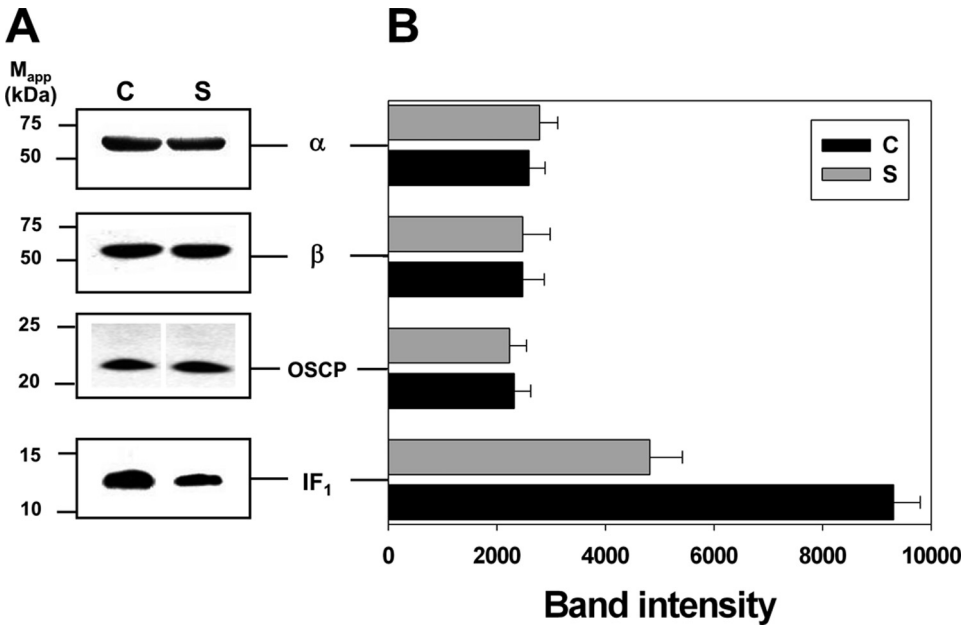

FIGURE 4. **Western blot analysis of complex V.** *A*, proteins from cytotrophoblast and syncytiotrophoblast mitochondria were resolved in an SDS-PAGE gel, and immunodetection of α, β, OSCP subunit, and F_0F_1-ATP synthase IF_1 was performed. The figure shows one representative experiment from seven human placentas processed. *C* and *S*, cytotrophoblast and syncytiotrophoblast mitochondria, respectively. *B*, densitometric analysis from Western blot shown in *A*. Statistical analyses showed a significant increase of the IF_1 band intensity in cytotrophoblast mitochondria when compared with syncytiotrophoblast, whereas α, β, and OSCP subunit intensities were similar in both mitochondria. A Student's *t* test indicates that the differences between cytotrophoblast and syncytiotrophoblast mitochondria are statistically significant ($p = 0.0005$, $n = 7$). *Error bars* indicate S.D.

estimate the complex V dimer/monomer ratio from Coomassie Brilliant Blue R-125-stained α and β subunits. The localization and MS identification of α and β in the two-dimensional SDS-PAGE (Fig. 3*C*, *spots 2* and *3*) confirmed that the ATP synthase extracted from cytotrophoblast mitochondria exists in roughly equal amounts in dimeric and monomeric forms (Fig. 3*C*, *left panel*); in contrast, in syncytiotrophoblast mitochondria, only trace amounts of the F_0F_1 dimer was observed, and the monomeric ATP synthase was therefore highly enriched (Fig. 3*C* and Table 2). These results suggest that in syncytiotrophoblast mitochondria, the ATP synthase exists preferably in the monomeric state.

It has been proposed that dimerization of the F_0F_1-ATP synthase plays an important role in mitochondrial cristae formation (11, 19–21). In mammalian mitochondria, the dimer of complex V is stabilized by the IF_1 (12). In this sense, the atypical mitochondrial morphology observed in syncytiotrophoblast cells could be associated with a diminished IF_1 content. To assess this possibility,, Western blot analyses of IF_1, α, β, and OSCP subunits were carried out in cytotrophoblast and syncytiotrophoblast mitochondria (Fig. 4*A*). Densitometry analysis showed that the relative signal of α, β, and OSCP subunits was similar in both cytotrophoblast and syncytiotrophoblast mitochondria; however, the relative intensity of IF_1 signal is on average twice as high as in cytotrophoblast than in syncytiotrophoblast mitochondria (Fig. 4*B*). Although the actual IF_1/complex V stoichiometries cannot be estimated by these densitometry analyses, the results are consistent with the hypothesis that a higher concentration of IF_1 in the cytotrophoblast cells results in larger amounts of F_0F_1-ATP synthase dimers, which in turn will promote the formation of mitochondrial cristae.

DISCUSSION

The present work shows that in common with mammalian, plant, and fungi mitochondria, human cytotrophoblast and syncytiotrophoblast mitochondria exhibit association of individual respiratory complexes into supercomplexes. When these organelles were solubilized with digitonin, a low amount of monomeric complex I was obtained, suggesting that *in vivo*, most of complex I is sequestered into supercomplexes. In addition, complex IV and III_2 associate with complex I into respirasomes; however, more than half of complex IV is in the monomeric free form, suggesting the existence an excess of cytochrome *c* oxidase. In cytotrophoblast and syncytiotrophoblast mitochondria, there was no evidence of the interaction of complex II with other proteins, although associations disrupted or not resolved by BN-PAGE cannot be ruled out. No significant differences were observed in the formation of respirasomes of cytotrophoblast and syncytiotrophoblast mitochon-

FIGURE 3. **In-gel activity and identification of digitonin-solubilized mitochondrial OXPHOS complexes from cytotrophoblasts and syncytiotrophoblasts in native gels.** Mitochondria were solubilized using digitonin (1.5 g/g of protein), and respiratory complexes were separated by BN-PAGE and CN-PAGE. Native-PAGE was performed onto linear polyacrylamide gradient gels from 5 to 10% (*A*) or from 3.25 to 7.5% (*B*). The *left panel* shows the Coomassie Brilliant Blue R-125-stained native gel strips. Assignment of complexes and assays were as in Fig. 2. The *right panel* shows the CN-PAGE and the ATPase activity assay (*A*). Bovine heart mitochondria were solubilized with digitonin as described under "Experimental Procedures" and used as standard. *B*, *C*, and *S* represent bovine, cytotrophoblast, and syncytiotrophoblast mitochondria, respectively; *CI*, *CII*, *CIV*, and *CV* correspond to in-gel catalytic activity assays of complexes I, II, IV, and V. Each complex subunit from cytotrophoblast and syncytiotrophoblast mitochondrial digitonin-solubilized supercomplex was resolved after the first BN-PAGE by two-dimensional SDS-PAGE (*C*), and its identity was determined using MALDI-TOF technique (indicated by molecular mass values shown in Table 2).

dria; however, significant differences were found in complex V dimerization, as discussed below.

The most significant observation of this work shows that the ATP synthase dimer is present in digitonin extracts of cytotrophoblast mitochondria but that it is scarce in syncytiotrophoblast mitochondria. This result is consistent with the presence of orthodox mitochondrial cristae in the former and the lack of cristae in the latter. It is well documented that complex V dimerization is a key element in the formation of tubular mitochondrial cristae (11, 19–21), and our correlation of a higher content of ATP synthase dimer in cytotrophoblast mitochondria is therefore in accordance with the role of ATP synthase dimer in cristae biogenesis. Furthermore, a critical role in the stability of the dimeric complex V has been proposed for its intrinsic inhibitor, IF_1. bovine, and rat IF_1 dimerize in solution (43). However, yeast IF_1 is less prone to dimerize (44). This different dimerizing propensity correlates well with the more prominent role of bovine and rat IF_1 in stabilizing the F_1 (45) and F_0F_1 dimers (12) when compared with the apparent dispensability of yeast IF_1 to dimerize F_0F_1 (26). Given the known dimerizing role of animal or human IF_1, we looked for an increase in IF_1 expression in cytotrophoblast over syncytiotrophoblast mitochondria that will correlate with the higher cristae content in the former model. In this line, the relative band intensities as developed by Western blot of IF_1 when compared with F_1 subunits (α, β, and OSCP) from cytotrophoblast and syncytiotrophoblast mitochondria were estimated. The blots showed a similar expression of the F_1 moiety in both cell types. In contrast, a reproducible increase in IF_1 expression relative to F_1 in cytotrophoblast *versus* syncytiotrophoblast was revealed by the intensity ratios of IF_1/F_1 subunits (α, β, or OSCP). The IF_1/α intensity ratios were 3.6 and 1.7 for cytotrophoblast and syncytiotrophoblast, respectively (Fig. 4). Although it is not possible to estimate a true IF_1/F_1 stoichiometry from Western blot data, the increase in IF_1/F_1 intensity ratios obtained shows an average 2-fold increase in IF_1 expression (relative to F_1) in cytotrophoblast mitochondria when compared with the syncytiotrophoblast model. A question therefore emerges as to the extent to which a 2-fold increase in IF_1 expression might affect mitochondrial cristae morphology. Previously, some of us had shown that a 2-fold increase in rat IF_1/F_1 expression in tumor AS-30D cells led to a higher association of IF_1 with the native F_0F_1 complex (46). Accordingly, this work shows the actual interaction of IF_1 with both monomeric and dimeric human F_0F_1 in cytotrophoblast mitochondria by MS identification in two-dimensional SDS-PAGE after BN-PAGE (Fig. 4). Similarly, an average 2.5-fold increase in IF_1/β expression as obtained by transient transfection of HeLa cultured cells with IF_1 led to a major increase in mitochondrial cristae density *in situ* (47). These results indicate that a 2-fold increase in IF_1 expression may be able to exert significant and evident changes in mitochondrial morphology as those observed here between cytotrophoblast and syncytiotrophoblast mitochondria. Accordingly, excess IF_1 also promotes oligomerization of the ATP synthase in addition to stabilizing the F_0F_1 dimer (12). Furthermore, recent three-dimensional structure of dimeric yeast ATP synthase suggests that the oligomerizing effect of excess IF_1 may take place at dimer-dimer interfaces of a diagonal ATP synthase oligomer wrapping mitochondrial cristae (35). Ongoing work[3] is assessing the effect of higher IF_1/F_1 overexpression ratios on cristae morphology. Meanwhile, it is important to note that other factors such as supernumerary F_0 subunits or different lipid composition (including cholesterol or steroid content, see below) besides IF_1 may also contribute to the differences in cristae morphology.

Although many types of mitochondrial cristae structure have been described (45), it is evident from recent electron microscopic tomography studies that there are differences between typical mitochondria and those from steroidogenic tissues. In general, cristae from typical mitochondria are a mixture of tubular and lamellar structures (48, 49), whereas in steroidogenic cells, cristae are tubular, vesicular, or tubulovesicular (50, 51). It has been suggested that due to this particular morphology of the cristae, mitochondria of Leydig cells should not be able to produce ATP because the narrow gap between lamellae would not allow the location of the F_1 moiety of the ATP synthase (50). However, recent data indicate that mitochondrial membrane potential ($\Delta\Psi m$), mitochondrial ATP synthesis, and mitochondrial respiration are all required to support Leydig cell steroidogenesis (52). Furthermore, in steroidogenic syncytiotrophoblast mitochondria, ATP is essential for progesterone synthesis (30). Accordingly, this work shows that both types of isolated mitochondria (steroidogenic and non-steroidogenic) exhibit similar rates of oxygen uptake coupled to ATP synthesis (Table 1). However, to correlate the mitochondrial cristae architecture with the rates of ATP synthesis, further work with intact mitochondria *in situ* rather than with isolated mitochondria will be needed.

Because the human placenta does not express Steroidogenic Acute Regulatory protein (StAR) (40) and Translocator protein (TSPO) (53) proteins involved in mitochondrial cholesterol flow, it has been suggested that the reduction in the size of syncytiotrophoblast mitochondria and the change in the structure of the cristae may improve the steroidogenic activity of the syncytiotrophoblast cells (27). The translocation of cholesterol to P450scc has long been known to be the rate-limiting step in steroidogenesis; thus, the greater surface to volume ratio could improve the movement of cholesterol to the inner membrane where the P450scc is located. This suggests that the non-orthodox cristae structure in mitochondria from steroidogenic tissue allows the cholesterol flow from the outer to the inner mitochondrial membranes and improves the hormone production. Because placental progesterone synthesis by syncytiotrophoblast mitochondria is required to suppress maternal uterine contractions to maintain pregnancy, the non-orthodox mitochondrial architecture of syncytiotrophoblast mitochondria may play a role in supporting sufficient progesterone synthesis to prevent spontaneous abortion (54). Syncytiotrophoblast mitochondria may lack cristae because these organelles

[3] J. J. García-Trejo, M. A. Valdéz-Solana, X. Pérez-Martínez, and C. Chávez-Castañeda, unpublished observations.

are specialized in progesterone production and may in part dispense with ATP synthase dimerization and oligomerization by reducing IF_1 expression.

Acknowledgments—We greatly appreciate the gift of heart bovine mitochondria from Professor Marietta Tuena de Gómez Puyou (Instituto de Fisiología Celular, Universidad Nacional Autónoma de México). We give our thanks to Dr. Juan Luis Rendón Gómez (Facultad de Medicina, Universidad Nacional Autónoma de México) and to Professor Andrew J. Rodgers from Commonwealth Scientific and Industrial Research Organisation (CSIRO) Molecular and Health Technologies, Clayton, Victoria, Australia, for the critical review of the manuscript.

REFERENCES

1. Saffman, P. G., and Delbrück, M. (1975) *Proc. Natl. Acad. Sci. U.S.A.* **72,** 3111–3113
2. Rich, P. R. (1984) *Biochim. Biophys. Acta* **768,** 53–79
3. Lenaz, G. (2001) *FEBS Lett.* **509,** 151–155
4. Schägger, H., and Pfeiffer, K. (2000) *EMBO J.* **19,** 1777–1783
5. Schäfer, E., Seelert, H., Reifschneider, N. H., Krause, F., Dencher, N. A., and Vonck, J. (2006) *J. Biol. Chem.* **281,** 15370–15375
6. Eubel, H., Heinemeyer, J., Sunderhaus, S., and Braun, H. P. (2004) *Plant Physiol. Biochem.* **42,** 937–942
7. Stroh, A., Anderka, O., Pfeiffer, K., Yagi, T., Finel, M., Ludwig, B., and Schägger, H. (2004) *J. Biol. Chem.* **279,** 5000–5007
8. Schägger, H. (2002) *Biochim. Biophys. Acta* **1555,** 154–159
9. Morales-Ríos, E., de la Rosa-Morales, F., Mendoza-Hernández, G., Rodríguez-Zavala, J. S., Celis, H., Zarco-Zavala, M., and García-Trejo, J. J. (2010) *FASEB J.* **24,** 599–608
10. Boekema, E. J., and Braun, H. P. (2007) *J. Biol. Chem.* **282,** 1–4
11. Minauro-Sanmiguel, F., Wilkens, S., and García, J. J. (2005) *Proc. Natl. Acad. Sci. U.S.A.* **102,** 12356–12358
12. García, J. J., Morales-Ríos, E., Cortés-Hernandez, P., and Rodríguez-Zavala, J. S. (2006) *Biochemistry* **45,** 12695–12703
13. Arnold, I., Pfeiffer, K., Neupert, W., Stuart, R. A., and Schägger, H. (1998) *EMBO J.* **17,** 7170–7178
14. Thomas, D., Bron, P., Weimann, T., Dautant, A., Giraud, M. F., Paumard, P., Salin, B., Cavalier, A., Velours, J., and Brèthes, D. (2008) *Biol. Cell* **100,** 591–601
15. Dudkina, N. V., Heinemeyer, J., Keegstra, W., Boekema, E. J., and Braun, H. P. (2005) *FEBS Lett.* **579,** 5769–5772
16. Cano-Estrada, A., Vázquez-Acevedo, M., Villavicencio-Queijeiro, A., Figueroa-Martínez, F., Miranda-Astudillo, H., Cordeiro, Y., Mignaco, J. A., Foguel, D., Cardol, P., Lapaille, M., Remacle, C., Wilkens, S., and González-Halphen, D. (2010) *Biochim. Biophys. Acta* **1797,** 1439–1448
17. Vázquez-Acevedo, M., Cardol, P., Cano-Estrada, A., Lapaille, M., Remacle, C., and González-Halphen, D. (2006) *J. Bioenerg. Biomembr.* **38,** 271–282
18. Rexroth, S., Meyer Zu Tittingdorf, J. M., Schwassmann, H. J., Krause, F., Seelert, H., and Dencher, N. A. (2004) *Biochim. Biophys. Acta* **1658,** 202–211
19. Allen, R. D. (1995) *Protoplasma* **189,** 1–8
20. Gavin, P. D., Prescott, M., Luff, S. E., and Devenish, R. J. (2004) *J. Cell Sci.* **117,** 2333–2343
21. Paumard, P., Vaillier, J., Coulary, B., Schaeffer, J., Soubannier, V., Mueller, D. M., Brèthes, D., di Rago, J. P., and Velours, J. (2002) *EMBO J.* **21,** 221–230
22. Arselin, G., Giraud, M. F., Dautant, A., Vaillier, J., Brèthes, D., Coulary-Salin, B., Schaeffer, J., and Velours, J. (2003) *Eur. J. Biochem.* **270,** 1875–1884
23. Arselin, G., Vaillier, J., Salin, B., Schaeffer, J., Giraud, M. F., Dautant, A., Brèthes, D., and Velours, J. (2004) *J. Biol. Chem.* **279,** 40392–40399
24. Brunner, S., Everard-Gigot, V., and Stuart, R. A. (2002) *J. Biol. Chem.* **277,** 48484–48489
25. Everard-Gigot, V., Dunn, C. D., Dolan, B. M., Brunner, S., Jensen, R. E., and Stuart, R. A. (2005) *Eukaryot. Cell* **4,** 346–355
26. Dienhart, M., Pfeiffer, K., Schagger, H., and Stuart, R. A. (2002) *J. Biol. Chem.* **277,** 39289–39295
27. Martínez, F., Kiriakidou, M., and Strauss, J. F., 3rd (1997) *Endocrinology* **138,** 2172–2183
28. Bensadoun, A., and Weinstein, D. (1976) *Anal. Biochem.* **70,** 241–250
29. Lowry, O. H., Rosebrough, N. J., Farr, A. L., and Randall, R. J. (1951) *J. Biol. Chem.* **193,** 265–275
30. Flores-Herrera, O., Uribe, A., García-Pérez, C., Milán, R., and Martínez, F. (2002) *Biochim. Biophys. Acta* **1585,** 11–18
31. Kao, L. C., Caltabiano, S., Wu, S., Strauss, J. F., 3rd, and Kliman, H. J. (1988) *Dev. Biol.* **130,** 693–702
32. Schägger, H., Cramer, W. A., and von Jagow, G. (1994) *Anal. Biochem.* **217,** 220–230
33. Wittig, I., and Schägger, H. (2007) *Methods Cell Biol.* **80,** 723–741
34. Wittig, I., Karas, M., and Schägger, H. (2007) *Mol. Cell. Proteomics* **6,** 1215–1225
35. Couoh-Cardel, S. J., Uribe-Carvajal, S., Wilkens, S., and García-Trejo, J. J. (2010) *J. Biol. Chem.* **285,** 36447–36455
36. González-Zamorano, M., Mendoza-Hernández, G., Xolalpa, W., Parada, C., Vallecillo, A. J., Bigi, F., and Espitia, C. (2009) *J. Proteome Res.* **8,** 721–733
37. Olivera, A. A., and Meigs, R. A. (1975) *Biochim. Biophys. Acta* **376,** 426–435
38. Cherradi, N., Defaye, G., and Chambaz, E. M. (1994) *Endocrinology* **134,** 1358–1364
39. Brand, C., Cherradi, N., Defaye, G., Chinn, A., Chambaz, E. M., Feige, J. J., and Bailly, S. (1998) *J. Biol. Chem.* **273,** 6410–6416
40. Tuckey, R. C. (1992) *J. Steroid Biochem. Mol. Biol.* **42,** 883–890
41. Wittig, I., Carrozzo, R., Santorelli, F. M., and Schägger, H. (2007) *Electrophoresis* **28,** 3811–3820
42. Wittig, I., and Schägger, H. (2005) *Proteomics* **5,** 4338–4346
43. Gordon-Smith, D. J., Carbajo, R. J., Yang, J. C., Videler, H., Runswick, M. J., Walker, J. E., and Neuhaus, D. (2001) *J. Mol. Biol.* **308,** 325–339
44. Cabezon, E., Butler, P. J., Runswick, M. J., Carbajo, R. J., and Walker, J. E. (2002) *J. Biol. Chem.* **277,** 41334–41341
45. Cabezón, E., Arechaga, I., Jonathan, P., Butler, G., and Walker, J. E. (2000) *J. Biol. Chem.* **275,** 28353–28355
46. Bravo, C., Minauro-Sanmiguel, F., Morales-Ríos, E., Rodríguez-Zavala, J. S., and García, J. J. (2004) *J. Bioenerg. Biomembr.* **36,** 257–264
47. Campanella, M., Casswell, E., Chong, S., Farah, Z., Wieckowski, M. R., Abramov, A. Y., Tinker, A., and Duchen, M. R. (2008) *Cell Metab.* **8,** 13–25
48. Mannella, C. A., Buttle, K., Rath, B. K., and Marko, M. (1998) *Biofactors* **8,** 225–228
49. Mannella, C. A., Pfeiffer, D. R., Bradshaw, P. C., Moraru, II, Slepchenko, B., Loew, L. M., Hsieh, C. E., Buttle, K., and Marko, M. (2001) *IUBMB Life* **52,** 93–100
50. Prince, F. P. (2002) *Mitochondrion* **1,** 381–389
51. Reichert, A. S., and Neupert, W. (2002) *Biochim. Biophys. Acta* **1592,** 41–49
52. Allen, J. A., Shankara, T., Janus, P., Buck, S., Diemer, T., Hales, K. H., and Hales, D. B. (2006) *Endocrinology* **147,** 3924–3935
53. Maldonado-Mercado, M. G., Espinosa-García, M. T., Gómez-Concha, C., Monreal-Flores, J., and Martinez, F. (2008) *Int. J. Biochem. Cell Biol.* **40,** 901–908
54. Miller, W. L. (1998) *Clin. Perinatol.* **25,** 799–817